PHYSICAL REVIEW B VOLUME 3, NUMBER 6 15 MARCH 1971

Determination of the Angular Dependence of the Specularity Parameter by Means of the Magnetic Field Dependence of the Magnetomorphic Oscillations*

Stephen B. Soffer†
Department of Physics, Polytechnic Institute of Brooklyn, Brooklyn, New York 11201
(Received 2 March 1970)

The specularity parameter used to describe the size effects in the electrical and galvanomagnetic transport properties of thin samples may depend on the angle of incidence of the electrons with the surface. It is difficult to determine this angular dependence experimentally because of the lack of reproducibility of surface preparation. A method is proposed to accomplish this with a single sample by means of a study of the details of the magnetomorphic oscillations (MMO) in the transverse galvanomagnetic properties. The magnetic field dependence of the amplitude of these oscillations contains information about the specularity parameter and its angular variation, especially for electrons normally incident to the surface. Existing data for Cd are analyzed from this standpoint. The higher-order terms introduced in this analysis are found to be responsible for the anomalous behavior of the MMO in Cd. The results are consistent with a highly anisotropic specularity parameter which may be caused by a surface-damage layer.

I. INTRODUCTION

A. Surface Scattering of Conduction Electrons

The scattering of conduction electrons at the surface of a metal has generally been studied by means of the size effects in the transport properties of thin films. In the theories of Fuchs[1] and Sondheimer,[2] the surface boundary condition has been incorporated by means of the specularity parameter p, which is defined as the probability an electron incident upon the surface will be scattered specularly. More recent theories[3,4] have indicated that the specularity parameter, if it is a reasonable description, is likely to be dependent on the angle of incidence of the electrons with the surface. The angular dependence can cause considerable alteration in the thickness dependence of the size effects from predictions based on a constant parameter.[4] Until the details of the surface scattering of electrons is understood the use of transport properties in thin films as a probe of bulk and surface properties will not reach its full potential.

B. Experimental Difficulties

So far there has apparently been no reliable quantitative experimental method developed for determining the angular dependence of p. One can measure the electrical resistivity in a thin film as a function of the thickness-to-mean-free-path ratio to try to determine this dependence. This ratio can be varied by changing either the thickness, or the mean free path through the temperature dependence. However, both these methods lead to difficulties in interpretation. In the former, either a new sample must be prepared or the thickness changed by adding or removing material. Aside from changes in the bulk properties it is very difficult to guarantee that the surface at each thickness remains the same. Since the transport properties are sensitive to the specularity parameter, which may in turn be sensitive to surface preparation, the specularity parameter could not be controlled. In the latter method, the same sample could be used. However, an adequate model for the directional and temperature dependence of the mean free path is hard to obtain because of sensitivity to static imperfections, especially at lower temperatures.

Other experimental measurements are affected by surface scattering. These include the anomalous skin effect, cyclotron resonance, and microwave absorption in weak magnetic fields.[5] The theory of these effects is fairly complicated and apparently has only been worked out for a constant specularity parameter for the first two. The theory, in the last effect, is relatively crude with respect to surface scattering, and other effects may dominate the line widths. However, recent work[6] has shown that correlation to surface preparation is attainable, with at least qualitative agreement with the predicted effect of surface roughness.[4]

Because of these difficulties in measuring the angular dependence of p, it would be desirable to have a method based on the relatively sensitive and theoretically simple transport size effects, but involving only a single sample, in which the bulk and, more importantly, the surface properties remain constant. We describe here how information can be obtained about the angular dependence of p under these conditions by studying the magnetomorphic oscillations (MMO) in the galvanomagnetic transport properties of conductors. As an illustration of the method, some existing experimental data are analyzed by this approach.

II. THEORY

The MMO were first predicted by Sondheimer.[2] Their relation to Fermi surface curvature has been studied by Gurevich.[7] Generally, diffuse surface scattering has been assumed. Recently, Mackey and Sybert[8] (MS) pointed out that the effect of partial specularity is to produce harmonics of the fundamental (Sondheimer) MMO. Physically, this may be visualized as equivalent to increasing the effective thickness of the sample by integral multiples of the actual thickness for those electrons which are not diffusely scattered on the first reflection. The relative amplitudes of the harmonics may be used to determine p, if it is assumed to be constant. Schwarz[9] has reported observing the second harmonic in Cd.

Here we extend the approach of MS to the case where the specularity parameter depends on the angle. First, the conductivity tensor is calculated using a simple Fermi-surface geometry. This is done in two ways, each giving different views of the effect of p's angular dependence on the MMO. The relative advantages and drawbacks of each view are discussed. The relation between the magnetic field dependence of the resistivity-tensor components and the angular dependence of p is given.

A. Discrete and Continuous Spectrum of the MMO

For this view of the problem we consider the simple parabolic-band model, in which each band of holes or electrons is in the "standard form"[10] and is assumed to have a constant scalar effective mass m. The size effects in the galvanomagnetic conductivities in the Sondheimer model may be written in the complex form

$$\sigma_c = \sigma_{11} + i\sigma_{12} = \sigma_c^0(B)[1 + I], \tag{1a}$$

$$I = -\frac{3}{2s}\int_1^\infty dw\,(w^{-3} - w^{-5})[1 - p(w)](1 - e^{-ws}) \times [1 - p(w)e^{-ws}]^{-1}, \tag{1b}$$

$$\sigma_c^0(B) = \sigma_{11}^0(B) + i\sigma_{12}^0(B) = \sigma^0[1 - i\omega\tau]/[1 + (\omega\tau)^2], \tag{1c}$$

$$\sigma^0 = ne^2\tau/m. \tag{1d}$$

Here the Sondheimer model has been made more general with the inclusion of the dependence of p on angle θ with the surface normal via $w = 1/\cos\theta$. The relaxation time is τ, the number density of carriers is n, and the cyclotron angular frequency is $\omega = eB/m$. The quantity $s = K + i\beta$, where $K = t/l$, t being the sample thickness and l the bulk mean free path, and $\beta = t/r$, r being the extremal orbit cyclotron radius v/ω, with v the velocity. The quantities r and β are signed, being positive (negative) for holes (electrons). In the following they will be treated as positive quantities, for convenience, unless specific reference is made to electrons. The zero superscript refers to bulk conductivities. More generally, these conductivities may be summed over bands if interband scattering is not too important.

The appearance of the MMO, including harmonics, can be shown in the conductivities as in MS by expanding the quantity $[1 - p(w)e^{-ws}]^{-1}$ in a geometric series. The expression I which contains all the size effects becomes

$$I = \bar{I} + \sum_{q=1}^{\infty} I_q, \tag{2a}$$

$$\bar{I} = -\frac{3}{2s}\int_1^\infty dw\,(w^{-3} - w^{-5})[1 - p(w)], \tag{2b}$$

$$I_q = \frac{3}{2s}\int_1^\infty dw\,(w^{-3} - w^{-5})[1 - p(w)]^2 p^{q-1}(w)e^{-qws}, \qquad q = 1, 2, 3, \ldots . \tag{2c}$$

The term $\bar{I}$ is monotonic in magnetic field and the integrands of I_q contain oscillations $e^{-iq\beta w}$. The effect of the dependence of p on angle can be shown by rewriting Eq. (2c). The result, shown in Appendix A, is

$$I_q = \frac{3}{2s}\left(F_q(1)\,\mathcal{E}(wqs)_{w=1} + \int_1^\infty dw\,\mathcal{E}(wqs)\frac{\partial F_q(w)}{\partial w}\right), \tag{3a}$$

$$F_q(w) = [1 - p(w)]^2 p^{q-1}(w), \tag{3b}$$

$$\mathcal{E}(wz) = w^{-2}E_3(wz) - w^{-4}E_5(wz), \tag{3c}$$

where $E_n(wz)$ is the exponential integral.[11] The reason for writing I_q in this form is that the second term of Eq. (3a) contains the effect of an angle dependent p. The asymptotic form of the exponential integrals[11] shows that the function defined in (3c) contains the oscillations $e^{-iq\beta w}$. From this viewpoint the magnetoconductivity size effect appears as having three kinds of field-dependent contributions. The purely monotonic part is $\bar{I}$. The first part of (3a) substituted in (2a) gives a series of harmonics with monotonically field-dependent amplitudes. This may be viewed as a *discrete spectrum* of the MMO. Finally, the second term of (3a) may be thought of as a *continuous spectrum* of the MMO. From this viewpoint, the presence of a continuous spectrum would indicate the presence of angular variation of p and give a measure of this variation.

Although this viewpoint has the advantage of separating out the effect of angular variation of sur-

face scattering, it has the drawbacks of being expressed in terms of an integral and, in the present case, being limited to the parabolic model.

B. Inverse Field Expansion of the MMO

Here we consider an alternative formulation. It essentially expresses the oscillatory magnetoconductivity as a power series in B^{-1} multiplying the oscillatory terms. By looking at the approach to high fields, the amplitude of the leading terms can be related to the angular dependence of p for limiting point electrons.

Grenier, Efferson, and Reynolds (GER), [12] as well as MS, have used this method to the lowest order in B^{-1}. We consider here also higher-order terms, since these lead to the angular dependence of p.

MS use a geometry developed by GER in which the Fermi surface is a figure of rotation about the magnetic field and sample-surface normal and has a reflection plane parallel to the sample surface. The parabolic-band model will be used here, although the method can easily be extended to the geometry of GER.

We expand the quantity

$$\tilde{I}=\sum_{q=1}^{\infty} I_q$$

as a series in β^{-1}. If one lumps all quantities in Eq. (2c) other than $F_q(w)\,e^{-iq\beta w}$ into the function $G_q(w)$, integration by parts yields [noting $G_q(w)$ and all its derivatives vanish at $w=\infty$]

$$\sum_{q=1}^{\infty}\int_1^{\infty} dw\,F_q(w)\,G_q(w)\,e^{-iq\beta w}$$

$$=\sum_{q=1}^{\infty} e^{-iq\beta}\sum_{r=1}^{\infty}(iq\beta)^{-r}\left(\frac{d^{r-1}}{dw^{r-1}}\left[F_q(w)\,G_q(w)\right]\right)_{w=1}$$

$$=\sum_{q=1}^{\infty} e^{-iq\beta}\{(iq\beta)^{-2}F_q(1)\,G_q'(1)$$

$$+(iq\beta)^{-3}\left[F_q(1)\,G_q''(1)+2F_q'(1)\,G_q'(1)\right]+\cdots\} \qquad (4)$$

(primes devoting d/dw). The last form occurs because $G_q(1)=0$. The quantity $F_q(w)$, as defined before, describes the surface scattering, whereas the function $G_q(w)$ depends only on quantities like Fermi surface, sample geometry, and magnetic field, but not on surface scattering.

In order to get them in a useful form the entire conductivities should be expanded in powers of B^{-1}. In general, the resulting expressions are quite complicated and the effects of p and its derivative come in, mixed together at the same order. However, a considerable simplification results by making an assumption which is in accordance with readily attainable experimental parameters. We will use the parameters defined in the parabolic-band model, although the results apply to the more general case with modifications in details. A useful identity is

$$\omega\tau=\beta/K=l/r\ . \qquad (5)$$

We will consider the region in which

$$\omega\tau\gg\beta>1\ . \qquad (6)$$

This is seen to require $K\ll 1$. Ideally, $\omega\tau$ should be as large as possible and β large enough to see a few oscillations, K being as small as possible. [These values are obtainable in high-purity crystals at liquid-helium temperatures, in high-field conventional or superconducting electromagnets. Typical values attainable are $l\approx 1$ mm, $\omega\tau\approx 10$ at 10 kG, and $t\approx 100\ \mu$. This gives $K\approx 10^{-1}$, $\beta\approx 1$ at this field. At higher fields (≈ 100 kG), still thinner samples could be used. Thinner samples are generally advantageous because of the $e^{-t/l}$ dependence of the voltages of interest.] The bulk part of $\bar{\sigma}$ depends only on $\omega\tau$. The size-dependent part of $\bar{\sigma}$ depends [Eq. (2b)] only on $\omega\tau$ and β, since

$$s=K+i\beta=i\beta\left[1-i(\omega\tau)^{-1}\right]\ .$$

The expansion may be expressed in terms of power series in $(\omega\tau)^{-1}$ and in β^{-1}. We will take the attitude that the condition (6), with K sufficiently small, allows keeping only the leading term of the $(\omega\tau)^{-1}$ series, but still requires considering several terms of β^{-1} to be important. The resistivity components may also be found by inversion. We shall assume a sample and Fermi-surface geometry of symmetry no lower than that of GER and MS. In this case the resistivities for the transverse effects are given simply by

$$\rho_{11}=\sigma_{11}/(\sigma_{11}^2+\sigma_{12}^2)\ , \qquad (7a)$$

$$\rho_{21}=\sigma_{12}/(\sigma_{11}^2+\sigma_{12}^2) \qquad (7b)$$

for the magnetoresistivity ρ_{11} and Hall resistivity ρ_{21}.

The details are given in Appendix B, taking for an example the transverse magnetoresistivity and the Hall resistivity in a single-band material, using the parabolic model. The results are easily extended to a multiband uncompensated material. [13] After expanding in powers of $(\omega\tau)^{-1}$, keeping leading terms, and then expanding in β^{-1}, the monotonic and oscillatory parts of the resistivity are

$$\bar{\rho}_{11}=-\rho^0\omega\tau(b\beta^{-1}-b^2\beta^{-3}+\cdots)\ , \qquad (8a)$$

$$\tilde{\rho}_{11}=-\rho^0\omega\tau[\tilde{c}_2'\beta^{-3}+(\tilde{c}_3'-2b\tilde{c}_2'')\beta^{-4}+\cdots]\ , \qquad (8b)$$

$$\bar{\rho}_{21}=-\rho^0\omega\tau(1-b\beta^{-2}+b^4\beta^{-4}+\cdots)\ , \qquad (8c)$$

$$\tilde{\rho}_{21}=\rho^0\omega\tau[\tilde{c}_2''\beta^{-3}+(2b\tilde{c}_2'+\tilde{c}_3'')\beta^{-4}+\cdots]\ , \qquad (8d)$$

where $\rho^0 = (\sigma^0)^{-1}$ is the zero-field resistivity and b, $\tilde{c}_n'$ and $\tilde{c}_n''$ are defined by

$$\bar{I} = b/(K + i\beta) , \tag{9a}$$

$$\tilde{I} = \sum_{q=1}^{\infty} I_q = (K + i\beta^{-1}) \sum_{n=2}^{\infty} \tilde{c}_n \beta^{-n} , \tag{9b}$$

$$\tilde{c}_n = \sum_{q=1}^{\infty} c_n^q e^{-iq\beta} = \tilde{c}_n' + i\tilde{c}_n'' . \tag{9c}$$

The coefficients c_n^q are found by applying Eq. (4) to $\tilde{I} = \sum I_q$. We note that $p(1)$ enters first via $\tilde{c}_2$, and $p'(1)$ first via $\tilde{c}_3$. Also, knowledge of b allows determination of $p(1)$ for given band geometry. Thus it is possible to get $p(1)$ from either a monotonic term $\propto B^0$ or B^{-1}, or an oscillatory term $\propto B^{-2}$. In a more general model there will also be a bulk term $\propto B^0$ in $\bar{\rho}_{11}$. However, $p'(1)$ requires an oscillatory term $\propto B^{-3}$.

At high fields, the first term in $\tilde{\sigma}_{11} + i\tilde{\sigma}_{12}$ goes as B^{-4} at high fields, as in MS. However, what this analysis shows in addition is that the anisotropy of the surface scattering shows up as a contribution to the oscillatory conductivity going as B^{-5} through the appearance of $F_q'(1)$ which contains $p'(1)$. In a model for the effect of surface roughness, [4] for a situation where the specularity parameter for normal incidence is of an intermediate value, $p(1) \approx \frac{1}{2}$, this derivative is reasonably large. However, the viewpoint of this kind of measurement should be to treat $p(1)$ and $p'(1)$ as unknown quantities to be determined. Later, the relationship to surface preparation may be considered.

The physical significance of the importance of the apex ($w = 1$) can be seen from the kinetic viewpoint. At high fields only electrons traveling nearly normal to the surface do not greatly increase their trajectory due to spiraling about the magnetic field. Thus, only these have a sufficiently small probability of scattering internally to contribute to the size effect, which is basically due to surface scattering. The microwave absorption method complements this one since there the angular variation near grazing incidence is observed. [5,6]

The two viewpoints presented each have advantages and disadvantages. The "discrete-continuous" view is easily adapted to arbitrary fields and gives information about scattering at angles other than normal incidence. However, it requires fitting data by an integral rather than a few terms of a series. Also, the present calculation is limited to parabolic bands. The B^{-1} expansion allows using the high-field region and the approach to high fields to extract the surface scattering from the band-dependent parts. It can be used with a somewhat more general band model.

The main advantage of the second viewpoint is that it shows explicitly, if the band model is known, how the specularity parameter and its angular derivative at normal incidence can be deduced from a study of the B dependence of the oscillatory conductivity without preparing a new surface or reducing thickness.

The limitation to bands with rotational and inversion symmetry, or even to the parabolic model in the present calculations, may not necessarily preclude application to real materials in certain cases. Band calculations have shown that even for a complicated Fermi surface, having segments in several zones, the free-electron model gives a fairly good description for points in wave-vector space which are not too close to a zone boundary. For example, in Zn the third-band disk has a largely free-electron curvature. [14] If the magnetic field and surface normal are parallel to normals to such segments of the Fermi surface, the "ineffectiveness" of other parts of the Fermi surface makes at least the oscillatory conductivity amenable to description by the simpler models.

III. EXPERIMENTAL EVIDENCE FOR HIGHER-ORDER MMO

A. Comparison of Data to Theory

Results of measurements of MMO in the Hall resistivity of a Cd crystal plate have been given by Mackey, Sybert, and Fielder (MSF). [15] A crystal, originally spark machined, was electropolished (100 μ per surface) to remove the spark-damaged layer. Additional planing and electropolishing were used to produce various thicknesses. In one case, abrasion was tried. The magnetic field and the thin dimension were parallel to the c axis.

The data are analyzed by using the high-field approximation

$$\tilde{\rho}_{21} \simeq \bar{\rho}_{11}^2 \sigma_{12}, \tag{10}$$

which is valid if $\bar{\rho}_{11}$ may be written as

$$\bar{\rho}_{11} = \alpha B^2. \tag{11}$$

This is true for the range of fields used and is to be expected for a compensated metal. MSF make the comparison to the theory as introduced in MS by keeping only the leading term of the β^{-1} expansion. From this, one predicts $\tilde{\rho}_{21}$ should oscillate as $\sin\beta$ and have a constant amplitude. In fact, the MSF data show a falling off of amplitude with β at higher fields for the thinner samples. More puzzling, as mentioned by MSF, is that the phases of the MMO are off by about $\frac{1}{2}\pi$ from the theory. This would imply, if constant amplitude is assumed, that $\tilde{\rho}_{21} \propto \cos\beta$. Since the standard procedure of field reversal and taking one-half the difference is employed, this would violate the requirement that $\tilde{\rho}_{21}$ must be odd in B. Similar behavior was re-

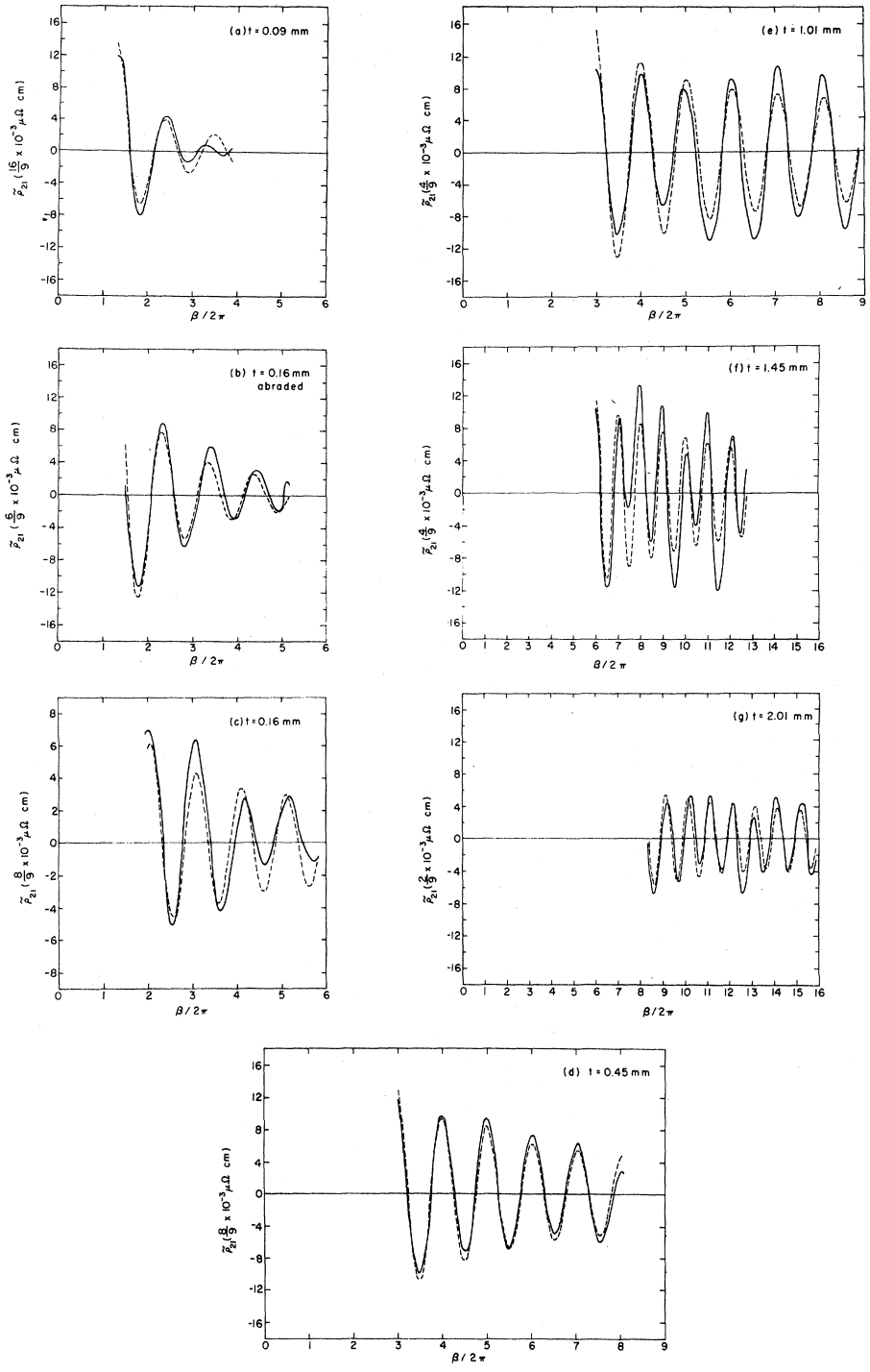

FIG. 1. Typical results of fitting the data (solid curves) of MS (Ref. 18) by the three-term expression, Eq. (21) (dashed curve). The case using the maximum number of data points for each thickness is given.

ported recently in cylindrical Cd samples.[16]

These apparent discrepancies are resolved if one considers higher-order terms in the β^{-1} expansion to be important. The reported periods are close to those predicted by the free-electron model. Also, nearly-free-electron calculations have shown the third-zone electrons to have nearly the free-electron curvature for the limiting point.[17] On this basis it will be assumed in the following analysis that the local conductivity producing the MMO is described by the free-electron model for a single band of electrons (although $\bar{\rho}_{11}$ should be described by the general multiband compensated expression). If one substitutes Eqs. (10) and (11) into Eq. (B3b), it is easily seen that the high-field form ($\omega\tau \gg 1$) of $\tilde{\rho}_{21}$ expanded in powers of β^{-1} may be written as

$$\tilde{\rho}_{21} = a_1 \sin|\beta| + a_2(\cos|\beta|)/|\beta| + a_3(\sin|\beta|)/|\beta|^2 + a_4(\cos|\beta|)/|\beta|^3 + \cdots . \quad (12)$$

[The magnitude of β has been written to facilitate comparison with experimental data. It will be assumed that electrons are responsible for the MMO so that β is negative. The coefficients of Eq. (12) are affected accordingly.] The higher-harmonic terms have been neglected, primarily on the basis of visual inspection of the $\tilde{\rho}_{21}$-vs-β curves. Further justification of this will be discussed below.

A least-squares fit was performed using the first three terms of Eq. (12). The results are shown in Fig. 1. The coefficients are given in Table I. In general, the fit is quite good for the thinner samples. For the thicker samples, presumably the smaller signal-to-noise ratios are responsible for a looser fit. However, in all cases the phase of the data is fitted quite closely by Eq. (12), and in most cases is close to that of $\cos\beta$. Calculations of a_1, $a_2/|\beta|$, and $a_3|\beta|^2$ show that in most cases the second term tends to be dominant. Thus it appears that it is the second-highest-order term proportional to $\cos\beta/\beta$ that is responsible for both the phase and the decreasing amplitude found in much of the MSF data. This also preserves the required odd symmetry.

It is of interest to see what values of $p(1)$, $p'(1)$, and $p''(1)$ follow from the empirically determined coefficients. The analysis is carried out as an illustration of the method. The results should be regarded as being of perhaps only qualitative significance. However, it is felt that, being a first attempt to apply the method, it is worthwhile following through to the consequences.

In order to determine $p(1)$, $p'(1)$, and $p''(1)$, the values of empirically determined coefficients of Eq. (12) are related to the theoretical expression (B3b), with multiplication by $\bar{\rho}_{11}^2 = \alpha^2(t) b^4(t) \beta^4$, where $B = b(t)|\beta|$ converts from magnetic field to phase variable. It would be desirable to determine the value of $\alpha(t)$ empirically. However, these were not available except for the thinnest sample. From MSF Fig. 5, $\alpha(0.09) = 10^{-2}\,\mu\Omega\,\mathrm{cm/kG^2}$. It has been found for Zn, which has a band structure very similar to Cd, that the thickness dependence of $\bar{\rho}_{11}$ was fitted reasonably well by the semiempirical expression

$$\alpha(t) = a/(1 + 3/8K), \quad (13)$$

although this is strictly based on a parabolic-band model.[13] This is employed here as a means for estimating $\alpha(t)$. The coefficients $b(t)$ follow from the periods $\Delta(t)$ by

$$b(t) = \Delta(t)/2\pi. \quad (14)$$

The bulk conductivity was calculated, assuming local

TABLE I. Results of analysis of data of MSF (Ref. 18) according to Eq. (12). The resultant coefficients a_1, a_2, and a_3 are given with the resultant values of $p(1)$, $p'(1)$, and $p''(1)$ and the ratios of second-to-first harmonic amplitudes $a_2^{(2)}/a_1^{(1)}$ consistent with these values. The few cases resulting in imaginary $p(1)$ are omitted.

t (mm)	Initial β $(\frac{2}{14})\pi$	No. of points	a_1 ($\mu\Omega$ cm)	a_2 ($\mu\Omega$ cm)	a_3 ($\mu\Omega$ cm)	$p(1)$	$p'(1)$	$p''(1)$	$a_1^{(2)}/a_1^{(1)}$	$a_2^{(2)}/a_2^{(1)}$	$a_3^{(2)}/a_3^{(1)}$
0.16	49	24	0.00203	−0.0465	−0.844	0.865	0.466	−1.78	1.53	0.364	0.103
abraded											
0.16	28	54	0.00153	0.0636	0.0992	0.883	−1.480	7.98	1.80	−0.0794	0.438
0.16	35	47	0.00169	0.0590	0.00310	0.877	−1.35	4.18	1.70	−0.101	−14.30
0.45	42	72	0.00261	0.209	−1.62	0.800	−5.67	84.2	0.882	0.0436	0.0255
0.45	49	65	0.00177	0.213	−1.33	0.812	−6.08	120	0.952	0.0474	0.0429
0.45	56	68	0.00195	0.215	−1.59	0.803	−5.87	96.5	0.896	0.0452	0.0288
0.45	63	51	0.00332	0.221	−3.81	0.743	−4.87	1.69	0.636	0.0315	0.00279
1.01	42	83	0.00212	0.126	−1.45	0.561	−7.57	14.2	0.240	0.0167	−0.0559
1.01	49	76	0.00224	0.134	−1.65	0.549	−7.81	11.5	0.228	0.0158	−0.0557
1.45	84	95	0.000218	0.190	−1.44	0.787	−47.0	9.65×10^3	0.609	0.0531	0.111
1.45	98	81	0.000897	0.192	−4.30	0.567	−24.2	776	0.216	0.0249	−0.0643
1.45	112	67	0.00111	0.216	−4.97	0.519	−24.6	667	0.178	0.0193	−0.0731
1.45	126	53	0.000265	0.223	−0.712	0.764	−50.0	10.0×10^3	0.536	0.0506	0.0514
1.45	140	39	0.00289	0.214	−15.3	0.223	−16.3	−492	0.0473	−0.0189	−0.0338
2.01	118	105	0.000537	0.0376	1.55	0.486	−10.3	357	0.133	0.00774	0.0178
2.01	142	81	0.000659	0.0429	0.682	0.431	−10.7	200	0.106	0.00265	0.0497
2.01	166	57	0.00116	0.0534	−3.21	0.243	−10.6	−295	0.0452	−0.0172	−0.0246

applicability of the free-electron model:

$$\sigma^0 = ne^2 l/\hbar\, k_F, \tag{15a}$$

$$n = k_F^3/3\pi^2. \tag{15b}$$

The appropriate Fermi wave vector k_F is 1.41 Å^{-1} for Cd. Comparing the resultant expression for $\tilde{\rho}_{21}$ with Eq. (12),

$$a_1 = 3K(t)e^{-K}[1-p(1)]^2, \tag{16a}$$

$$a_2 = -K(t)e^{-K}\{3[1-p(1)]^2(9+2K) + 12[1-p(1)]p'(1)\}, \tag{16b}$$

$$a_3 = -K(t)e^{-K}(3[1-p(1)]^2(75+27K+3K^2) + 18[1-p(1)]p'(1)(9+2K) + 18\{[p'(1)]^2 + [1-p(1)]p''(1)\}), \tag{16c}$$

where $K(t) \equiv \sigma^0\alpha^2(t)b^4(t)K$. These can be solved for $p(1)$, $p'(1)$, and $p''(1)$, the results being given in Table I. In addition, these values can be used to calculate the coefficients of the higher harmonics to check whether their neglect is justified. The second-harmonic expressions corresponding to Eq. (16) are

$$a_1^{(2)} = \tfrac{3}{4}K(t)e^{-2K}[1-p(1)], \tag{17a}$$

$$a_2^{(2)} = \tfrac{1}{8}K(t)e^{-2K}(6\{[1-p(1)]^2 - 2[1-p(1)]\}p'(1) - 3[1-p(1)]p(1)(9+4K)), \tag{17b}$$

$$a_3^{(2)} = -\tfrac{1}{16}K(t)e^{-2K}(3[1-p(1)]p(1)(75+54K+12K^2) - 9\{[1-p(1)]^2 - 2[1-p(1)]p(1)\}p'(1)(9+4K) + 9\{[6p(1)-4][p'(1)]^2 + [1-p(1)][1-2p(1)]p''(1)\}). \tag{17c}$$

The numerical results are given in Table I. In most cases the second harmonic is comparable to the corresponding first harmonic only for the leading term. For the dominant second term it is usually much smaller. Neglecting second harmonics may cause some error in the determination of $p(1)$, and therefore of $p'(1)$ and $p''(1)$ also. The relatively large sizes of $p'(1)$ and $p''(1)$ also restrict the accuracy of the expansion to small region about the normal. Thus the remaining results of this analysis must be considered as possibly only approximate. A more involved analysis, using six equations, would be required if the second harmonic is really significant. Its relatively small contribution makes it seem unlikely that it is.

The results for $p(1)$, $p'(1)$, and $p''(1)$ show some degree of systematic thickness variation, in spite of scatter and some nonmonotonic behavior. In general, as the thicknesses are reduced, $p(1)$ increases somewhat, then remains relatively constant. $p'(1)$ is negative and decreases in magnitude with diminishing t. $p''(1)$ is positive and decreases by several orders of magnitude with reduction. In the one case for the abraded sample, $p(1)$ is negligibly changed, but $p'(1)$ has become a small positive quantity and $p''(1)$ has also changed sign. A plot of the specularity parameter versus angle for small angles with respect to the normal, calculated from the approximate expansion

$$p(w) = p(1) + p'(1)(w-1) + \tfrac{1}{2}p''(1)(w-1)^2, \tag{18}$$

is given in Fig. 2. Because of the possibly limited region of validity, only the vicinity of the normal is likely to be accurate.

B. Discussion of Possible Relation to the Nature of the Surface

Although more precision would be desirable, it is possible to make some inferences as to the relationship between the surface scattering near normal incidence and the nature of the surface region.

If the dominant mechanism for nonspecular surface scattering is cancellation of scattered waves caused by random tangentially uncorrelated surface-position variations, the specularity parameter has a predicted angular dependence of

$$p(\theta) = e^{-\Gamma/w^2}, \tag{19}$$

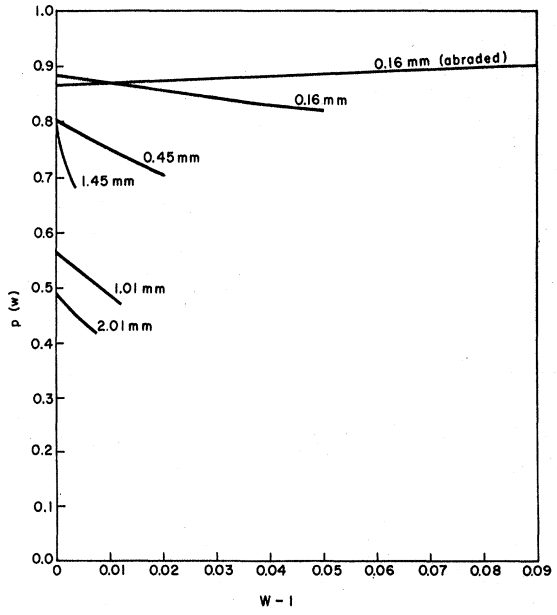

FIG. 2. Typical angular variation of the specularity parameter of Cd according to the data of MSF (Ref. 18), for angles of incidence near the surface normal, using Eq. (20). The expansion coefficients are from Table I.

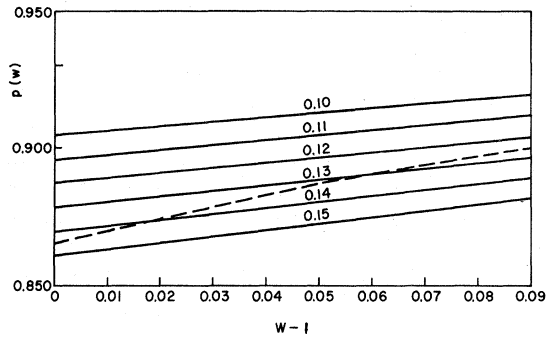

FIG. 3. Comparison of the angular dependence of the specularity parameter (dashed curve) for the abraded case of MSF (Ref. 17) with the predictions of the statistical model (Ref. 4, solid curves). The abraded case is obtained as in Fig. 3. The statistical model is from Eq. (28). The roughness parameter is $\Gamma = (4\pi h/\lambda)^2$.

where $\Gamma = (4\pi h/\lambda)^2$, h being the rms surface-height variation and λ the de Broglie wavelength.[4]

Figure 3 shows low-angle-of-incidence evaluations of the statistical model, Eq. (19). In addition, the analysis by Eq. (18) of the abraded case is shown on the same graph. It is seen that, although no unique Γ describes this curve, the range of Γ is relatively small, indicating at least approximate agreement with the statistical model.

It is interesting to note that all other cases yield a negative $p'(1)$. This is inconsistent with the statistical model. Furthermore, for the thicker cases $p'(1)$ has a much larger magnitude than $p'(1)(\leq 2/e)$ that would be expected from this model. Thus it does not appear that the unabraded cases, especially the thicker ones, can be explained by a model in which the phase cancellation due to surface-height variations plays a major role.

The negative sign of $p'(1)$ along with its increasing magnitude with t suggests that a residual damage layer may be more effective than true surface scattering, especially in the thicker samples. Damage due to spark planing to depths of 100 μ have been reported.[18] It is possible that the initial electropolishing of this magnitude still did not entirely remove this layer, but that the additional 100 μ per surface removed for the thinner samples accounted for most of it. In fact, $-p'(1)$ shows a crudely exponential dependence on $t - t_0$, where t_0 is presumably of the order of the undamaged thickness whereas $p(1)$ only increases slightly with diminished thickness. The additional planing operations make this analysis somewhat oversimplified, however. The results suggest that presence of grain boundaries predominantly oriented perpendicular to the surface may serve as tunneling barriers for wave-vector components parallel to the surface with very little effect on the components perpendicular to it. The effect of abrasion may have been to produce some surface annealing, recrystallization, or other means of removal of residual-damage region, allowing more nearly true surface scattering to show up. Also, in addition to the effect of further planing, it is conceivable that electropolishing may tend to propagate some of the damage layer. Recent calculations have shown that grain-boundary scattering may dominate true surface scattering in polycrystalline thin films.[19]

IV. SUMMARY AND CONCLUSIONS

It has been shown that the spectrum of the MMO contains information about both the specularity parameter and its anisotropy. This can be extracted if the band structure is known. The main advantage of the approach is the lack of need for reproducibility in preparation of multiple samples or surfaces since p should be quite sensitive to small variations of the latter.

Cd data is analyzed and shows the presence of the higher-order terms that are needed to give information on angular dependence. The analysis, to the extent that second-harmonic contributions are negligible, points to a lack of true surface scattering, possibly due to a residual spark-damaged layer, except in an abraded sample.

These results indicate that this technique, for studying conduction electron-surface scattering and its relationship to surface preparation, appears promising. Future work should emphasize carefully controlled surface preparation and the observation of the correlation between this preparation and the resultant angular dependence of p. Also a more involved analysis, including second harmonics and still higher-order terms available from lower fields, might lead to a more accurate determination of $p(w)$, extending to a larger angle from the normal.

ACKNOWLEDGMENTS

I am grateful to Dr. Paul D. Hambourger and Dr. H. J. Mackey for correspondence concerning their work.

APPENDIX A

Equations (3) can be derived from Eq. (2c) by direct application of the definitons of differentiation and integration. However, it is easier to prove that (3) reduces to (2c). Integration by parts gives for the second term in the brackets of (3), setting $qs = z$,

$$J \equiv \int_1^\infty dw\, \mathcal{E}(zw)\frac{\partial F_q(w)}{\partial w}$$

$$= -\left[F_q(1)\mathcal{E}(zw)_{w=1} + \int_1^\infty dw\, F_q(w)\frac{\partial \mathcal{E}(zw)}{\partial w}\right].$$

Using the identity and recurrence relationship[11]

$$\frac{\partial E_n(zw)}{\partial z} = -zE_{n-1}(zw), \quad n = 1, 2, 3, \ldots$$

where

$$E_{n+1}(zw) = (1/n)[e^{-zw} - zwE_n(zw)], \quad n = 1, 2, 3, \ldots$$

it is straightforward to show

$$\frac{\partial E_n(zw)}{\partial w} = -(w^{-3} - w^{-5})e^{-zw} .$$

Substitution of this into J, and J into Eqs. (3), gives Eq. (2c).

APPENDIX B

Here we give a general expression for the complex conductivity in the parabolic model in terms of the inverse field-dependent quantities $\gamma \equiv (\omega\tau)^{-1}$ and $\delta \equiv \beta^{-1}$. Then assuming that

$$\gamma \ll \delta < 1 , \tag{B1}$$

we work out the resistivity tensor for monotonic and oscillatory field dependence as an expansion in powers of the inverse field. Using the quantities defined by Eqs. (9), it can be shown that

$$\sigma_c = \sigma^0\gamma(1-\gamma^2)^{-1}[-i+\gamma-e^{2i\gamma}f(\delta)], \tag{B2}$$

where

$$f(\delta) = f'(\delta) + if''(\delta),$$

$$f'(\delta) = b\delta + \sum_{n=2}^{\infty} \tilde{c}_n' \delta^{n+1},$$

$$f''(\delta) = \sum_{n=2}^{\infty} \tilde{c}_n'' \delta^{n+1} .$$

Expanding $(1+\gamma^2)^{-1}$ and $e^{2i\gamma}$ gives

$$\sigma_{11} = \sigma^0\gamma\{-f'(\delta) + [1+2f''(\delta)]\gamma + 5f'(\delta)\gamma^2 + \cdots\} ,$$

$$\sigma^{12} = \sigma^0\gamma\{-[1+f''(\delta)] - 2f'(\delta)\gamma + [1+5f''(\delta)]\gamma^2 + \cdots\} .$$

Using the restriction of (B1), keeping only leading terms of γ, we have

$$\sigma_{11} \cong -f'(\delta)\sigma^0\gamma , \tag{B3a}$$

$$\sigma_{12} \cong -[1+f''(\delta)]\sigma^0\gamma . \tag{B3b}$$

These results can be extended to a multiband model by summing over bands if there is no compensation. For compensated bands, the leading Hall-conductivity term cancels and the results must be modified. This is easily done[13] and is omitted here.

Inverting Eq. (10) and expanding in powers of δ,

$$\rho_{11} = -\rho^0\omega\tau[b\delta + \tilde{c}_2'\delta^3 + \tilde{c}_3'\delta^4 + \cdots]D(\delta) ,$$

$$\rho_{21} = -\rho^0\omega\tau[1 + \tilde{c}_2''\delta^3 + \tilde{c}_3''\delta^4 + \cdots]D(\delta) ,$$

where

$$D(\delta) = 1 - b^2\delta^2 - 2\tilde{c}_2''\delta^3 + (b^4 - 2b\tilde{c}_2' - 2\tilde{c}_3'')\delta^4 + \cdots .$$

Multiplication and grouping of terms, and separating monotonic and oscillatory parts, give Eqs. (8).

---

*Work supported in part by National Aeronautics and Space Administration Grant No. NsG-589, and Office of Naval Research Grant No. N00014-A0438-0005.

†Present address: Institut de Physique Expérimentale Université de Lausanne, Lausanne, Switzerland.

[1]K. Fuchs, Proc. Cambridge Phil. Soc. 34, 100 (1938).

[2]E. H. Sondheimer, Advan. Phys. 1, 1 (1952).

[3]R. F. Greene and R. W. O'Donnell, Phys. Rev. 147, 599 (1966).

[4]S. B. Soffer, J. Appl. Phys. 38, 1719 (1967).

[5]R. E. Prange and T. Nee, Phys. Rev. 168, 779 (1968).

[6]J. F. Koch and T. E. Murray, Phys. Rev. 186, 722 (1969).

[7]V. L. Gurevich, Zh. Eskperim. i Teor. Fiz. 35, 668 (1958) [Soviet Phys. JETP 8, 464 (1959)].

[8]H. J. Mackey and J. R. Sybert, Phys. Rev. 158, 658 (1967).

[9]H. Schwarz, Physik Kondensierten Materie 9, 164 (1969).

[10]See, e.g., A. H. Wilson, *The Theory of Metals* (Cambridge U. P., Cambridge, England, 1952), 2nd ed., p. 43.

[11]*Handbook of Mathematical Functions*, edited by M. Abromowitz and I. A. Stegun (U. S. Dept. of Commerce, Natl. Bur. Std., Washington, D. C., 1964), Appl. Math. Ser. 55, pp. 228–231.

[12]C. G. Grenier, K. R. Efferson, and J. M. Reynolds, Phys. Rev. 143, 406 (1966).

[13]S. B. Soffer, Phys. Rev. 176, 861 (1968).

[14]W. A. Harrison, Phys. Rev. 126, 497 (1962).

[15]H. J. Mackey, J. R. Sybert, and J. T. Fielder, Phys. Rev. 157, 578 (1967).

[16]H. J. Mackey, J. R. Sybert, and R. D. Hight, Phys. Rev. B 1, 2385 (1970).

[17]See, e.g., R. W. Stark and L. M. Falicov, Phys. Rev. Letters 19, 795 (1967) or Ref. 14.

[18]See, e.g., H. D. Guberman, J. Appl. Phys. 39, 2975 (1968).

[19]A. F. Mayadas and M. Shatzkes, Phys. Rev. B 1, 1382 (1970).